2015 International Symposium on Nonlinear Theory and its Applications
NOLTA2015, Kowloon, Hong Kong, China, December 1-4, 2015

Dynamic Behavior of Current-Controlled Full Bridge Inverter

Hiroki Kawano†, Takuji Kousaka‡ and Hiroyuki Asahara†

† Faculty of Engineering, Okayama University of Science,
1-1 Ridai-cho, Kita-ku Okayama-shi, Okayama 700-0005, Japan.
‡ Faculty of Engineering, Oita University,
700 Dannoharu, Oita-shi, Oita 870-1192, Japan.
Email: kawano@nonlineargroup.net, takuji@oita-u.ac.jp, asahara@ee.ous.ac.jp

Abstract—In the previous study, we have started to analyze the nonlinear phenomena in the current-controlled full bridge inverter under a practical circuit parameter using which the ac waveform of 60Hz is generated. However, the detail analysis of the circuit is insufficient. In this paper, we analyze the dynamic behavior of the circuit in more detail. First, we show the circuit model and the waveform behavior. Then, we define the discrete map of the fast- and slow-scale dynamics, respectively. Finally, we investigate the relationship between the fast- and slow-scale dynamics.

1. Introduction

Power converter circuits are used in many electrical equipment. Therefore, proposing the new circuit model, studying the circuit theory, improving the power conversion efficiency, etc. are important. Some of the power converter circuits have the switching devices and it causes the nonlinear phenomena. Analyzing the nonlinear phenomena in the power converter circuits can contribute to developing the circuit theory and be a help for understanding the dynamic behavior of the circuit in a wide parameter space. Therefore, there are many papers which study the nonlinear phenomena in the power converter circuits since 1990s [1, 2]. In recent years, it can be said that the nonlinear phenomena in the power converter circuits with low-dimensional topology are analyzed in detail [3, 4]. However, analyzing the nonlinear phenomena in the power converter circuits with high-dimensional topology or with complicated dynamics are insufficient.

This paper focuses on the current-controlled full bridge inverter. The circuit structure of the full bridge inverter is simple. However, the carrier signal and the reference sinusoidal signal, which is used for controlling the switching action, make the circuit dynamics complicated. In general, the waveform behavior observed in the time interval corresponding to the carrier signal is called as the fast-scale dynamics [5], whereas that of corresponding to the sinusoidal signal is called as the slow-scale dynamics [6]. Nonlinear phenomena observed in the fast- and slow-scale dynamics have been investigated in the previous study [7]. The previous studies analyzed the circuit with two or more dimensional topology. Therefore, for clarifying the basic property of the nonlinear phenomena observed in the fast- and slow-scale dynamics in detail, we have started to analyze the simple interrupted electric circuit in Refs. [8, 9, 10, 11]. In particular, Refs. [10, 11] analyzed the full bridge inverter with one dimensional topology. However, the circuit parameters was not practical in Ref. [10]. Although Ref. [11] improved the circuit parameter and analyzed the nonlinear phenomena observed in the fast- and slow-scale dynamics separately, the relationship between the fast- and slow-scale dynamics is not discussed.

In this paper, we deal with the relationship between the fast- and slow-scale dynamics in the full bridge inverter. First, we show the current-controlled full bridge inverter with one dimensional topology. Then, we explain the waveform behavior. Next, we define the discrete map of the fast- and slow-scale dynamics, respectively. Finally, we discuss the relationship between the fast- and slow-scale dynamics.

2. Current-controlled full bridge inverter

Figure 1 shows the circuit model, which is proposed in Ref. [12]. We have studied the nonlinear phenomena in the circuit in Ref. [13]. Moreover, we have improved the controller as shown in Fig. 2 in Ref. [10]. The nonlinear phenomena in the improved circuit were studied in Ref. [11].

In the following analysis, we shows circuit dynamics based on Ref. [11]. The circuit parameters are fixed as $E = 50$[V], $L = 1$[mH] and $R = 4.8$[Ω]. The circuit has four switches, where switch-1 (SW1) and switch-4 (SW4) being a pair. Likewise, switch-2 (SW2) and switch-

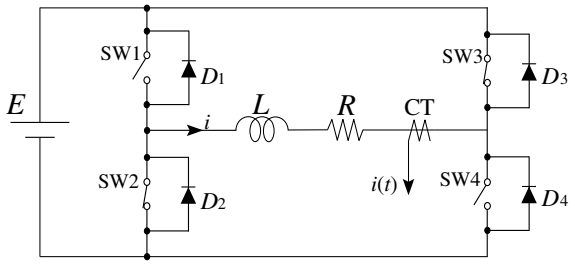

Figure 1: Full bridge inverter.

3 (SW3) being a pair. If SW1 (SW4) is ON and SW2 (SW3) is OFF, we call it as *state-A*, otherwise we call it as *state-B*. The switching signal u_n is as follows:

$$u_n = k\left(V_{\mathrm{ref}}^{\mathrm{s}}(nT_{\mathrm{f}}) - i_n\right), \tag{1}$$

where k is a gain of the controller, $V_{\mathrm{ref}}^{\mathrm{s}}(nT_{\mathrm{f}})$ and i_n denote the sampling data of the carrier signal and the inductance current at a time of $t = nT_{\mathrm{f}}$. Note that $n = 0, 1, 2, 3, \ldots$, and T_{f} denotes a period of the carrier signal, where $T_{\mathrm{f}} = 83.3[\mu s]$. Moreover, we use the following dimensionless variables.

$$i = \frac{E}{R}x,\ t = \frac{2L}{R}\tau,\ T_{\mathrm{f}} = \frac{2L}{R}T_{\mathrm{f}}',\ T_{\mathrm{s}} = \frac{2L}{R}T_{\mathrm{s}}' \tag{2}$$

Therefore, the circuit equation is derived as follows:

$$\frac{dx}{d\tau} = \begin{cases} -2(x-1), & \text{forstate} - \text{A} \\ -2(x+1), & \text{forstate} - \text{B} \end{cases}. \tag{3}$$

Note that $T_{\mathrm{s}} = NT_{\mathrm{f}}$ denotes the period of the reference sinusoidal signal, where $N = 200$. In the following analysis, we rewrite the variables T_{f}' and T_{s}' with T_{f} and T_{s}, for the sake of the simplicity. Therefore, the solution of Eq. (3) is derived as follows:

$$x(\tau) = \begin{cases} \varphi_{\mathrm{a}}(\tau, x_n, \lambda), & \text{forstate} - \text{A} \\ \varphi_{\mathrm{b}}(\tau, x_n, \lambda), & \text{forstate} - \text{B} \end{cases}, \tag{4}$$

where λ denotes a parameter. Note that x_n denotes an initial value of the inductance current at a time of $\tau = nT_{\mathrm{f}}$, where $n = 0, 1, 2, 3, \ldots, N-1$. Figure 3 shows the waveform behavior, where (a) shows a long time scale view, which we call the slow-scale dynamics and (b) shows a short time scale view, which we call the fast-scale dynamics. Note that the switching signals are shown in Fig. 3 (b). Here, let the minimum value of the carrier signal be 0, whereas maximum value of that is V_{U}. The circuit keeps state-B during a time that satisfies $u_n \le V_{\mathrm{ref}}^{\mathrm{f}}(\tau)$, otherwise the circuit keeps state-A. Therefore, the discrete map of the fast-scale dynamics is defined as follows:

$$\begin{aligned} x_{n+1} &= F_n(x_n) \\ &= \begin{cases} f_{\mathrm{i}} = \varphi_{\mathrm{a}}(T_{\mathrm{f}}, x_n, \lambda), & u_n \ge V_{\mathrm{U}} \\ f_{\mathrm{ii}} = \varphi_{\mathrm{b}}(T_{\mathrm{f}}, x_n, \lambda), & u_n \le 0 \\ f_{\mathrm{iii}} = \varphi_{\mathrm{b}}(\tau_{\mathrm{b}}, x(\tau_{\mathrm{a}}), \lambda) \circ \varphi_{\mathrm{a}}(\tau_{\mathrm{a}}, x_n, \lambda), & 0 < u_n < V_{\mathrm{U}} \end{cases}, \end{aligned} \tag{5}$$

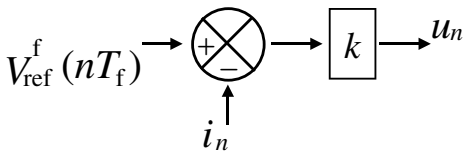

Figure 2: Control block.

where τ_{a} and τ_{b} denote a time during which the circuit keeps state-A and state-B, respectively. Likewise, the discrete map of the slow-scale dynamics is defined as follows:

$$\begin{aligned} x_{p+1} &= G(x_p) \\ &= F_{N-1} \circ \cdots \circ F_1 \circ F_0(x_p) \\ &= F_{N-1} \circ \cdots \circ F_1 \circ F_0(x_0) \end{aligned}. \tag{6}$$

Note that x_p denotes an initial value of the inductance current at a time of $\tau = pT_{\mathrm{f}}$ with $n = 0$, where $p = 1, 2, 3, \ldots$.

3. Analytical results

Figure 4 shows the waveform behaviors by changing the parameter k, which is the gain of the controller. It is clear that a bifurcation phenomenon occurs in the circuit by changing the parameter k. For example, a periodic solution can be observed at $k = 3.0$, while the non-periodic solutions are observed in the other parameter values of k. In the following analysis, we consider the bifurcation mechanism.

The stability of the fast-scale and slow-scale dynamics can be calculated based on the following equations:

$$\frac{dF_n(x_n)}{dx_n} - \mu_{\mathrm{f}} = 0, \tag{7}$$

$$\frac{dG(x_p)}{dx_p} - \mu_{\mathrm{s}} = 0, \tag{8}$$

where μ_{f} and μ_{s} denote the characteristic multipliers of the fast- and slow-scale dynamics, respectively. Note that

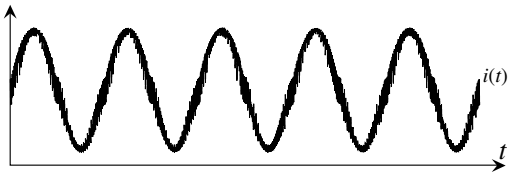

(a) Slow-scale dynamics

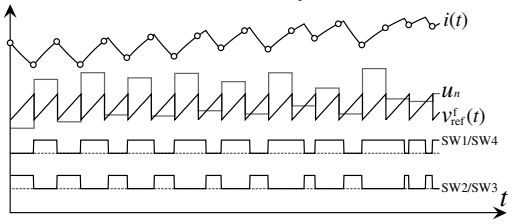

(b) Fast-scale dynamics

Figure 3: Waveform behavior.

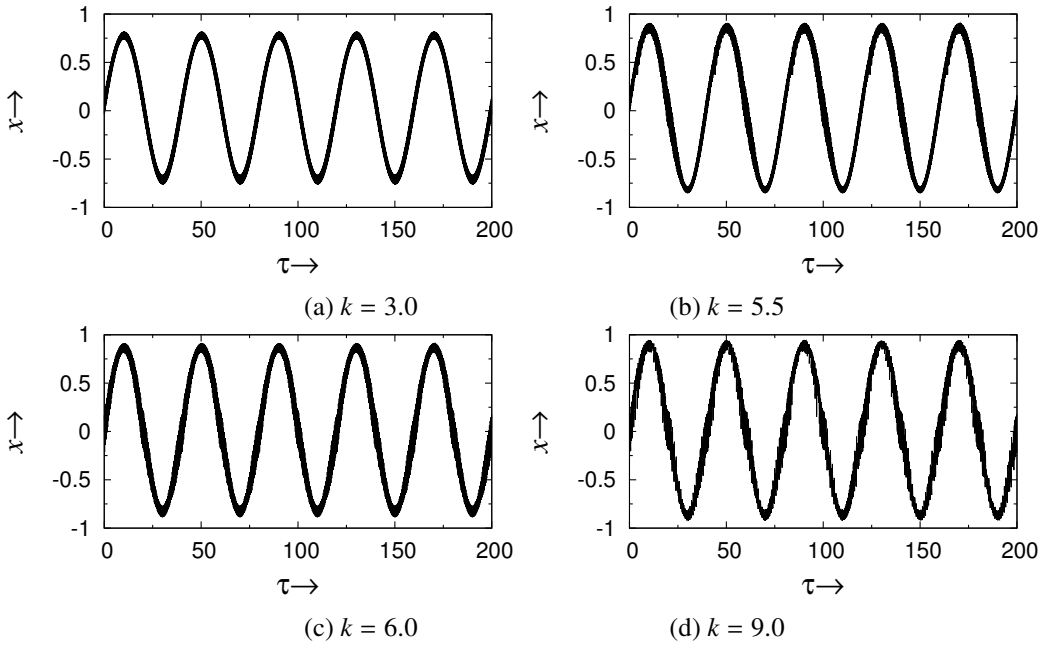

(a) $k = 3.0$ (b) $k = 5.5$

(c) $k = 6.0$ (d) $k = 9.0$

Figure 4: Waveforms in the slow-scale dynamics.

$dG(x_p)/dx_p$ is derived as follows:

$$\begin{aligned}\frac{dG(x_p)}{dx_p} &= \frac{dx_{p+1}}{dx_p} \\ &= \frac{dF_{N-1}}{dx_{N-1}} \cdots \frac{dF_1}{dx_1}\frac{dF_0(x_p)}{dx_p}, \\ &= \frac{dF_{N-1}}{dx_{N-1}} \cdots \frac{dF_1}{dx_1}\frac{dF_0(x_0)}{dx_0}\end{aligned} \tag{9}$$

If $|\mu_{\mathrm{f}}| < 1$ is satisfied, we regard that the fast-scale dynamics is approximately stable. Likewise, it is said that the slow-scale dynamics is stable if $|\mu_{\mathrm{s}}| < 1$ is satisfied.

Table 1 shows the stability calculation results with $T_{\mathrm{f}} = 0.2$. In the table, $\mu_{\mathrm{f}}^{\mathrm{M}}$ denotes the maximum value of the characteristic multiplier in the fast-scale dynamics within the one cycle of the slow-scale dynamics. It is clear that both the fast-scale dynamics and the slow-scale dynamics keep stable state at $k = 4.311$ and $k = 4.312$. On the other hand, a part of the fast-scale dynamics becomes unstable at $k = 4.313$ because $\left|\mu_{\mathrm{f}}^{\mathrm{M}}\right| > 1$ is satisfied. The slow-scale dynamics becomes unstable at $k = 6.64$. Therefore, it can be concluded that a part of the fast-scale dynamics becomes unstable, however, the slow-scale dynamics keeps stable oscillation during $4.313 \leq k \leq 6.63$. More complicated nonlinear phenomena may occurs during $4.313 \leq k \leq 6.63$.

4. Conclusion

This paper analyzed the nonlinear phenomena in the current-controlled full bridge inverter under a practical circuit parameter using which the ac waveform of 60Hz can be generated. First, the full bridge inverter was shown. Then, the control block was formed by using 12kHz of the sampling data of the carrier signal and the inductance current. The switching devices were controlled by output of the control block. Next, the discrete map of the fast- and slow-scale dynamics were defined. Finally, nonlinear phenomena in the circuit were shown by changing the parameter value of k, which is a gain of the controller. Moreover, stabilities of the fast- and slow-scale dynamics were calculated by using the discrete map. Based on the stability calculation results, the relationship between the fast- and slow-scale dynamics was discussed. It was found that the fast-scale dynamics became unstable and then the slow-scale dynamics became unstable by changing the bifurcation parameter of k. This characteristic may be the same with all of the current-controlled full bridge inverter. We consider that more interesting nonlinear phenomena can be observed in the parameter range in which a part of the fast-scale dynamics becomes unstable, whereas the slow-scale dynamics keeps stable oscillation.

In future, we will focus on the above parameter range and clarify the relationship between the fast- and slow-scale dynamics. Moreover, we will report the dynamical mechanism of the appearance of the harmonic distortion in the full inverter. The experimental investigation is also included in the future work.

Acknowledgment

This work was supported by JSPS KAKENHI Grant Number 26730134.

Table 1: Stability calculation results ($T_f = 0.2$)

k	μ_s	μ_f^M	Remarks
4.31100	0.00000	-0.99960	Stable fast-scale dynamics and stable slow-scale dynamics
4.31200	0.00000	-0.99999	Stable fast-scale dynamics and stable slow-scale dynamics
4.31300	0.00000	-1.00039	Unstable fast-scale dynamics and stable slow-scale dynamics
4.31500	0.00000	-1.00119	Unstable fast-scale dynamics and stable slow-scale dynamics
.	.	.	.
5.00000	0.00953	-1.27406	Unstable fast-scale dynamics and stable slow-scale dynamics
5.01000	0.01877	-1.27804	Unstable fast-scale dynamics and stable slow-scale dynamics
5.01068	0.01966	-1.27832	Unstable fast-scale dynamics and stable slow-scale dynamics
5.01100	0.02008	-1.27844	Unstable fast-scale dynamics and stable slow-scale dynamics
5.03000	0.07229	-1.28601	Unstable fast-scale dynamics and stable slow-scale dynamics
5.05000	0.27590	-1.29399	Unstable fast-scale dynamics and stable slow-scale dynamics
5.06000	0.53717	-1.29797	Unstable fast-scale dynamics and stable slow-scale dynamics
5.08000	0.02132	-1.35537	Unstable fast-scale dynamics and stable slow-scale dynamics
5.09000	-0.00443	-1.36055	Unstable fast-scale dynamics and stable slow-scale dynamics
.	.	.	.
6.60000	-0.89972	-1.96539	Unstable fast-scale dynamics and stable slow-scale dynamics
6.62000	0.83537	-1.97034	Unstable fast-scale dynamics and stable slow-scale dynamics
6.63000	-0.96308	-1.95823	Unstable fast-scale dynamics and stable slow-scale dynamics
6.64000	-2.13303	-1.97459	Unstable fast-scale dynamics and unstable slow-scale dynamics

References

[1] D.C. Hamill, D.J. Jefferies, "Subharmonics and chaos in a controlled switched-mode power converter," *IEEE Trans. Circuits and Syst. I,* vol, 35, pp. 1059-1061, 1988.

[2] J.H.B. Deane, D.C. Hamill, "Instability, subharmonics and chaos in power electronics systems," *IEEE Trans. Power Electron.,* vol. 5, no. 3, pp. 260-268, 1990.

[3] S. Banerjee, G.C. Verghese, eds, "Nonlinear phenomena in power electronics: Attractors, bifurcations, chaos, and nonlinear control," *IEEE Press,* 2001.

[4] C.K. Tse, "Complex behavior of switching power converters," *Boca Raton CRC Press,* 2003.

[5] M. Li, D. Dai, X. Ma and H.H.C. Iu, "Fast-scale period-doubling bifurcation in voltage-mode controlled full-bridge inverter," *IEEE International Symposium on Circuits and Systems,* pp. 2829–2832, 2008.

[6] M. Li, D. Dai and X. Ma, "Slow-scale and fast-scale instabilities in voltage-mode controlled full-bridge inverter," Circuits Syst. Signal Process., vol. 27, pp. 811–831, 2008.

[7] Y. Chen, C. K. Tse, S. Qiu and W. Schwarz, "Coexisting fast-scale and slow-scale instability in current-mode controlled DC/DC converters: analysis, simulation and experimental results," *IEEE Trans. Circuits Syst. I, Fundam. Theory Appl.,* vol. 55, no. 10, pp. 3335–3348, 2008.

[8] H. Asahara, K. Aihara and T. Kousaka, "Stability analysis of an interrupted circuit with fast-scale and slow-scale bifurcations," *Proc. of The IEEE 10th International Conference on Power Electronics and Drive Systems,* pp. 12–15, 2013.

[9] Y. Izumi, H. Asahara and T. Kousaka, "Basic study of border-collision bifurcation in an electric circuit including fast-scale and slow-scale dynamics," *Journal of Signal Processing,* vol. 18, no. 4, pp. 153–156, 2014.

[10] S. Shosui, T. Fujii, H. Asahara and T. Kousaka, "Qualitative behavior for simple H-bridge inverter," *Proc. of 2014 International Symposium on Nonlinear Theory and Its Applications,* pp. 890–893, 2014.

[11] H. Asahara, T, Kousaka, "Nonlinear oscillation in current-mode controlled dc/ac inverter," *Proc. of 8th Chaotic Modeling and Simulation International Conference,* 2015. (In press)

[12] B. Robert and C. Robert, "Border-collision bifurcation in a one-dimensional piecewise smooth map for a PWM current-programmed H-bridge inverter," *Int. J. Cont.,* vol. 75, pp. 1356–1367, 2002.

[13] H. Asahara and T. Kousaka, "Bifurcation analysis in a PWM current-controlled H-bridge inverter," *Int. J. Bifurcat. Chaos,* vol. 21, no. 3, pp. 985–996, 2011.